International Immunology Advance Access published December 9, 2008

International Immunology 2008; 1 of 17
doi:10.1093/intimm/dxn118

© The Japanese Society for Immunology. 2008. All rights reserved.
For permissions, please e-mail: journals.permissions@oxfordjournals.org

# Antagonism of CRTH2 ameliorates chronic epicutaneous sensitization-induced inflammation by multiple mechanisms

**Stefen A. Boehme[1], Edward P. Chen[1], Karin Franz-Bacon[1], Roman Šášik[2,3], L. James Sprague[2], Tai Wei Ly[1], Gary Hardiman[2,4]** and **Kevin B. Bacon[1]**

[1]Actimis Pharmaceuticals, Inc., 10835 Road to the Cure, Suite 200, San Diego, CA 92121, USA
[2]Biomedical Genomics Microarray Facility (BIOGEM), School of Medicine, [3]Moore's Cancer Center and [4]Department of Medicine, University of California, La Jolla, San Diego, CA, USA

*Keywords*: allergy, CRTH2, inflammation, prostaglandin $D_2$, skin

### Abstract

**Prostaglandin $D_2$ ($PGD_2$) and its receptor chemoattractant receptor homologous molecule expressed on $T_h2$ cells (CRTH2) have been implicated in the pathogenesis of numerous allergic diseases. We investigated the role of $PGD_2$ and CRTH2 in allergic cutaneous inflammation by using a highly potent and specific antagonist of CRTH2. Administration of this antagonist ameliorated cutaneous inflammation caused by either repeated epicutaneous ovalbumin or FITC sensitization. Gene expression and ELISA analysis revealed that there was reduced pro-inflammatory cytokine mRNA or protein produced. Importantly, the CRTH2 antagonist reduced total IgE, as well as antigen-specific IgE, IgG1 and IgG2a antibody levels. This reduction in antibody production correlated to reduced cytokines produced by splenocytes following *in vitro* antigen challenge. An examination of skin $CD11c^+$ dendritic cells (DC) showed that in mice treated with the CRTH2 antagonist, there was a decrease in the number of these cells that migrated to the draining lymph nodes in response to FITC application to the skin. Additionally, naive $CD4^+$ T lymphocytes co-cultured with skin-derived DC from CRTH2 antagonist-treated mice showed a reduced ability to produce a number of cytokines compared with DC from vehicle-treated mice. Collectively, these findings suggest that CRTH2 has a pivotal role in mediating the inflammation and the underlying immune response following epicutaneous sensitization.**

### Introduction

Prostaglandin $D_2$ ($PGD_2$) is the major prostenoid released by mast cells upon antigen activation. A pivotal role for $PGD_2$ has long been implicated in various allergic diseases in humans, such as allergic dermatitis, asthma and allergic rhinitis, as well as murine models of these disorders. For instance, elevated levels of $PGD_2$ have been found in the BAL fluid of patients after endobronchial antigen challenge (1, 2), and transgenic mice over-expressing lipocalin-type $PGD_2$ synthase showed an increase of $PGD_2$ in the lungs together with a concomitant increase of eosinophils and lymphocytes in response to an antigenic challenge (3). There are two known receptors for $PGD_2$, the D prostenoid receptor DP1 and chemoattractant receptor homologous molecule expressed on $T_h2$ cells (CRTH2). In humans, CRTH2 has been shown to be expressed by $T_h2$ lineage $T_h$ cells, eosinophils and basophils, and the mouse additionally expresses CRTH2 in a subset of $T_h1$ cells and bone marrow-derived mast cells (4; Stefen A. Boehme, unpublished results).

The role of CRTH2 in allergic inflammation has been controversial. Activation of CRTH2 by $PGD_2$ or the CRTH2-specific agonist 13,14-dihydro-15-keto-prostaglandin $D_2$ (DK-$PGD_2$) induces the chemotaxis of $T_h2$ cells, eosinophils and basophils and this was inhibited by ramatroban, a thromboxane A2 receptor antagonist that weakly cross-reacts with CRTH2 (5–7). Stimulation of human $T_h2$ cell lines with $PGD_2$ or DK-$PGD_2$ resulted in the production of IL-4, IL-5 and IL-13 (8, 9). DK-$PGD_2$ has also been shown to induce eosinophil migration to inflammatory sites in mouse models of atopic dermatitis (AD) and allergic asthma (10), as well as to induce human eosinophil degranulation (11). The experiments

*Correspondence to*: S. A. Boehme; E-mail: sboehme@actimis.com

*Transmitting editor*: K. Inaba

*Received* 27 June 2008, *accepted* 25 September 2008

utilizing gene-deficient mice, however, have been conflicting. Using CRTH2-deficient mice bred to a BALB/c background, Satoh *et al.* (12) showed that the mutant mice had a reduced inflammatory response in a number of mouse models of skin inflammation, along with depressed IgE levels. In contrast, a study of allergic airway inflammation using C57Bl/6 CRTH2 knockout mice showed increased eosinophil recruitment into the lung following antigen challenge (13). Another study using DP1-deficient mice reported increased serum IgE levels and a decreased inflammatory infiltrate of lymphocytes and eosinophils in the lungs of knockout animals compared with wild type (14). Gene compensatory mechanisms may explain some of the discrepancies observed in the various knockout mice, or the role of CRTH2–$PGD_2$ is fundamentally different in allergic inflammation of the skin versus airway inflammation. However, these studies taken in sum point out that the role of the CRTH2–$PGD_2$ interaction in an allergic inflammatory response *in vivo* is not fully understood.

AD is a chronic inflammatory skin disease characterized by severe pruritis, enhanced $T_h2$ responses, peripheral blood eosinophilia and elevated serum IgE levels. The majority of patients with AD develop asthma and/or allergic rhinitis later in life and a subset of patients also develop food allergies (15). Acute AD lesions show a mononuclear cell infiltrate consisting primarily of activated memory $CD4^+$ T cells, and to a lesser extent, macrophages and mast cells. Chronic lesions also show an infiltrate of eosinophils and $IgE^+$ Langerhans cells (16). It has been shown that the severity of AD correlates with an increased number of circulating $CRTH2^+$ cutaneous lymphocyte-associated antigen (CLA)-positive $T_h$ cells (17, 18). As IgE-mediated activation of mast cells results in $PGD_2$ secretion, these observations suggest a role for the $PGD_2$–CRTH2 system in the disease initiation and progression of AD. However, as is the case for allergic airway disease, the role of CRTH2 in skin inflammatory diseases such as AD has not been fully assessed.

Epicutaneous sensitization with allergens is thought to play an important role in the pathogenesis of AD. Similarly, chronic epicutaneous sensitization of mice with a protein antigen, chick egg ovalbumin (OVA), leads to the development of localized skin inflammation and this mouse model exhibits many of the characteristics of AD. For instance, the inflammatory infiltrate in this chronic model is composed primarily of T cells and eosinophils and local production of $T_h2$ cytokines, such as IL-4 and IL-5 as well as IFN-$\gamma$ and IL-17A (19–21). *In vitro* OVA challenge of draining lymph node (dLN) cells from epicutaneously immunized mice resulted in the production of IL-17A, IL-4 and IFN-$\gamma$ (20). In this study, skin-derived $CD11c^+$ dendritic cells (DC) were shown to play a key role in eliciting cytokine production by capturing antigen and migrating from the skin to the dLNs (20).

Here, we use a highly specific and potent small molecule antagonist of CRTH2 to investigate the role of this $PGD_2$ receptor in chronic models of cutaneous inflammation and the underlying immune response. Our results show that inhibition of CRTH2 leads to a decrease in the inflammatory infiltrate, locally produced pro-inflammatory cytokines and chemokines, as well as a reduction in antigen-specific antibodies. This reduction in antibody levels is mediated by CRTH2 and is associated with a decrease in cytokines produced in the spleen following epicutaneous immunization. Furthermore, this effect can be directly correlated with a decreased ability of skin DC from CRTH2-blocked mice to elicit cytokine production by naive T lymphocytes.

## Materials and methods

### *Materials*

All reagents were purchased from Sigma (St Louis, MO, USA) unless otherwise stated. The animal care and use committee (IACUC) approved all animal experimentation prior to implementation. All mice were purchased from The Jackson Laboratories (Bar Harbor, ME, USA) and were females 4–6 weeks of age. Compound A is a selective and proprietary CRTH2 antagonist developed at Actimis Pharmaceuticals, Inc. and is represented under patent WO2005/073234A3. Radioligand-binding assays demonstrated the $IC_{50}$ values of Compound A inhibiting $PGD_2$ binding to CRTH2 (using cells transfected with human or mouse CRTH2): murine CRTH2, 3.7 nM $IC_{50}$, human CRTH2, 4.5 nM. Compound A did not effectively antagonize other prostanoid, thromboxane or cysteinyl leukotriene receptors as the $IC_{50}$ values for Compound A inhibiting DP1, BLT1, CysLT1, CysLT2, EP1, EP2, EP3, EP4, FP, IP and TP are all >10 $\mu$M. Compound A displayed no activity on a large and diverse panel of G protein-coupled receptors as determined by a PanLabs screen (MDS Pharma, King of Prussia, PA, USA) (22). In 1-week FITC-induced ear swelling assays in mice, the $ED_{50}$ of Compound A was calculated to be ~0.13 mg $kg^{-1}$. Collectively, this biological and pharmacological profile of Compound A demonstrates that it is a highly potent and selective CRTH2 antagonist.

### *Epicutaneous sensitization of mice*

Epicutaneous sensitization of BALB/cJ mice was carried out as described previously (19). In brief, the mice were anaesthetized using isoflurane (TW Veterinary Supply, Lago Vista, TX, USA) and the dorsal skin was shaved. A $1 \times 1$ $cm^2$ section of gauze was soaked in either PBS (Mediatech, Herndon, VA, USA) or 1% ovalbumin (Fraction VI) solution (dissolved in PBS) and placed on the exposed dorsal skin. This was held in place using a transparent bioocclusive dressing (IV3000 MPV transparent dressing, Smith & Nephew, Largo, FL, USA). After the initial 3 days, a fresh patch was placed on the same area for a 4-day period; hence, each sensitization period was for a total of 7 days. For the chronic 50-day model described in Fig. 1, the mice received a total of three skin patchings, each for a 7-day period. There was a 2-week interval between the first and second patchings and second and third patchings. One day following the completion of third patching (day 50), the mice were sacrificed, serum was isolated following cardiac puncture (Microtainer Serum Separator Tubes, Becton Dickinson, Mountain View, CA, USA) and patched skin was harvested for histological, RNA and protein analysis. For RNA and protein analysis, the skin was snap frozen in a dry ice/liquid nitrogen bath and stored at −80°C until further processing. During these studies, mice were dosed daily with Compound A [10, 1 and 0.1 mg $kg^{-1}$ orally (p.o.)] during the second and third sensitization periods.

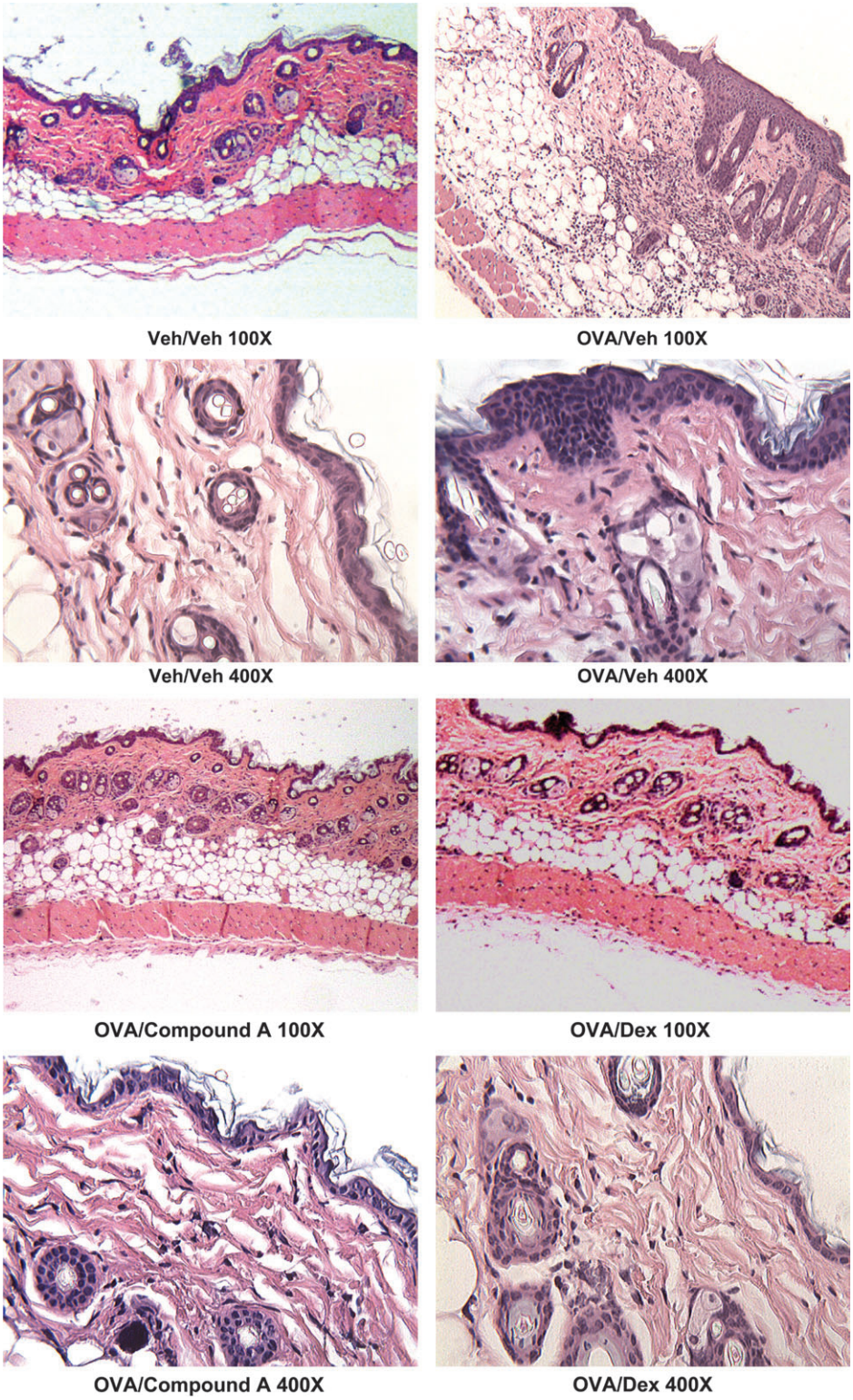


**Fig. 1.** BALB/c mice were epicutaneously sensitized with ovalbumin on the dorsal skin three times over a 50-day period and patched areas were examined by histology, mRNA expression and cytokine/chemokine levels. Serum was also isolated and antibody levels were determined (Figs 1–4). This figure shows the histology of patched skin sections from mice treated with PBS and drug vehicle, OVA and drug vehicle, OVA and Compound A (10 mg $kg^{-1}$) and OVA and dexamethasone (5 mg $kg^{-1}$) treatment. The skin sections were stained with hematoxylin and eosin and examined under ×100 and ×400 magnification. The OVA/veh-treated section shows epidermal thickening and a large inflammatory infiltrate in the dermis.

*Histological analysis*

For histological examination of patched skin, skin sections were excised 24 h after removal of the patch from the third sensitization. Specimens were fixed in 10% buffered formalin and embedded in paraffin. Multiple 4-μm sections were stained with hematoxylin and eosin. For spleen peanut agglutinin (PNA)-stained sections, spleens were frozen in OCT medium (Tissue Tech, Torrance, CA, USA) and a dry ice/isopentane bath, cut in 4-μm sections, and the slides were stained with biotinylated PNA (Vector Laboratories, Burlingame, CA, USA) and alkaline phosphate streptavidin and cover slipped using Vectashield mounting medium (Vector Laboratories). All slides were imaged using a Zeiss Primostar microscope (Zeiss MicroImaging, Thornwood, NY, USA), a Moticam 2000 camera and Motic Images Plus 2.0 software (Motic, Richmond, British Columbia, Canada).

*Specific antibody ELISA*

Serum was isolated at the indicated times by cardiac puncture or tail bleeding and assayed for either total IgE levels or antigen-specific antibody levels. Determination of total IgE was performed using the BD-Pharmingen kit following the instructions. Quantitation of OVA-specific antibodies was as follows; 96-well EIA/RIA flat-bottom plates (Costar, Corning, NY, USA) were coated with Fraction VI ovalbumin (50 μg OVA per milliliter of PBS, 100 μl per well) overnight, washed (PBS, Tween 20) and blocked for 1 h with 200 μl of 5% FCS (Lonza Biowhittaker, Portsmouth, NH, USA) and 1% BSA (Fraction V). The plates were washed and the diluted serum (5% FCS, 1% BSA was the dilution buffer) was added (100 μl per well) and incubated for 2 h at room temperature. For serum samples isolated on day 14 onward, the serum was diluted as follows for analysis of the different isotypes: IgE—1/20, IgG1—1/400 and IgG2a—1/200. Following washing, the biotinylated detection antibodies were added [anti-mouse IgE (clone R35-118, BD-Pharmingen, San Diego, CA, USA), anti-mouse IgG1 (clone A85-1, BD-Pharmingen) and anti-mouse IgG2a (clone R19-15, BD-Pharmingen)] together with the SA-HRP (BD-Pharmingen). After a 2-h incubation, the plates were washed and developed with peroxidase substrate reagents (BD-Pharmingen). The absorption at 405 nM was read with an automated plate reader (kinetic microplate reader; Molecular Devices, Sunnyvale, CA, USA). Antigen-specific antibody measurements were in the linear range of the standard curve and final quantitation of antigen-specific antibody was expressed in arbitrary units.

*Gene expression analysis*

Patched skin from mice treated with a PBS skin patch or an OVA skin patch ± Compound A treatment was excised on day 50, one after the third epicutaneous sensitization period. The skin sections were snap frozen in a dry ice/liquid nitrogen bath and stored at −80°C until RNA isolation. Total RNA was isolated using the Oligotex RNA isolation kit according to the manufacturer's directions (Qiagen Sciences, Valencia, CA, USA). Biotinylated cRNA was prepared using the Illumina RNA Amplification Kit according to the manufacture's instructions (Ambion Inc, Austin, TX, USA). The mRNA was converted to cDNA and then amplified and labeled by T7 DNA polymerase. The Illumina Mouse 6 Sentrix Expression BeadChip was used (Illumina, San Diego, CA, USA). Following hybridization and washing, the arrays were scanned on an Illumina BeadArray Reader. The signals were computed with weighted averages of pixel intensities, and local background was subtracted. Sequence-type signal was calculated by averaging corresponding bead signals from the three liver samples with outliers removed (median absolute deviation).

Simultaneous normalization of multiple microarrays was done using the 'mloess' method (23). Genes were ranked according to interest. In designing the interest statistic, we borrow ideas from Cole *et al.* (24) and their software package Focus. The interest statistic reflects a biologist's view that a gene with a greater fold change (in absolute value) than other genes is potentially the more interesting one. Also, given two genes with the same fold changes, it is the gene with a higher expression level (and therefore higher absolute change) that is the more interesting one. Genes were subsequently organized into functional groups and their expression patterns displayed as a heatmap.

Array data have been deposited in the EBI Array Express Database (accession number is pending).

*Quantitative real-time PCR analysis*

Relative mRNA transcript levels were measured by real-time quantitative reverse transcription–PCR in a LightCycler 480 (Roche Applied Science, Pleasanton, CA, USA). Total RNA reverse transcribed using the Roche Transcriptor kit (Roche Applied Science) and 50 ng cDNA was quantified using LightCycler 480 Probe Master kit (Roche Applied Science). Duplicate biological samples were used. Each sample was run as a technical duplicate and mean values were reported. Normalized gene expression values were obtained using LightCycler Relative Quantification software (Roche Applied Science). Relative gene copy numbers were derived by efficiency-corrected relative quantification using the formula $2^{\Delta CT}$ where $\Delta CT$ is the difference in amplification cycles required to detect amplification product from equal starting concentrations of RNA. The sequences of the oligonucleotide primers and the corresponding Universal Probe Library probe were supplied by Roche Applied Science. Results were expressed as fold change compared with PBS + vehicle-treated skin.

*Analysis of cytokine and chemokine levels in patched skin sections*

Patched skin sections were excised as described above and snap frozen in a dry ice/liquid nitrogen bath and stored at −80°C until analysis. Skin sections were then immersed in T-PER protein isolation buffer (Pierce, Rockford, IL, USA), containing freshly added protease and phosphatase inhibitors, and homogenized using an IKA ultra-turrax homogenizer (IKA Works, Inc., Wilmington, NC, USA). Solid contaminants (e.g. hair) were removed by centrifugation at 4°C, and the protein level in the supernatant was quantitated by a BCA Protein Quantitation Assay (Pierce). Cytokines or chemokines levels in the protein lysates were assessed by ELISA analysis, and 50 or 100 μg of protein was used per data point. ELISAs

were carried out in triplicate or duplicate, and the average ± SEM is shown. All ELISA kits were purchased from R&D Systems (Minneapolis, MN, USA), with the exception of IL-4, which was obtained from BD-Pharmingen. All ELISAs were used according to the manufacturer's protocol.

*Spleen cell culture*

Spleens were isolated from mice epicutaneously sensitized with PBS or 1% ovalbumin ± Compound A treatment (ovalbumin, Fraction VI, Sigma). Single-cell suspensions of splenocytes were cultured in 96-well round-bottom plates (Costar) at a concentration of $2 \times 10^6$ splenocytes per well in the presence of ovalbumin (100 μg $ml^{-1}$). After 72 h, supernatants were isolated and analyzed for cytokine expression by ELISA.

*Analysis of culture supernatants for cytokine production*

Culture supernatants were analyzed for cytokines and chemokines by ELISA analysis. All ELISAs, with the exception of IL-4, were purchased from R&D Systems. IL-4 ELISA was obtained from BD-Pharmingen. All ELISAs were used according to the manufacturer's directions.

*FITC-induced cutaneous inflammation*

A FITC-induced allergic inflammation model was carried as follows. The bellies of female BALB/cJ mice were shaved on days 1 and 14. On days 1, 2, 14 and 15, 400 μl of a 0.5% FITC solution was painted on the shaved ventral skin (dissolved in acetone:dibutyl phthalate, 1:1, v/v). Mice were p.o. dosed with Compound A (1 mg $kg^{-1}$) either daily from days 14 to 25 or day 25 only. FITC-sensitized control mice were dosed with drug vehicle on days 14–25. A control cohort of mice (Veh/veh) was sensitized with acetone:dibutyl phthalate with no FITC on days 1, 2, 14 and 15 and drug vehicle on day 25. On day 25, the mice were challenged with 0.5% FITC on the right ear (20 μl volume) or FITC vehicle only on the left ear (20 μl volume). The Veh/veh cohort received the FITC vehicle on both ears. Ear thickness of both ears was determined 24 h after the FITC challenge using a digital calipers (Fisher Scientific, Pittsburgh, PA, USA). The thickness of the left ear 24 h after FITC vehicle challenge was almost identical to values prior challenge (Stefen A. Boehme, unpublished results). Ear edema was expressed by thickness of the right (FITC-challenged ear) − thickness of the left ear. After the measurement of ear thickness at 24 h, blood was obtained by cardiac puncture and serum isolated for total IgE quantitation.

*Analysis of $CD11c^+$ dendritic cells*

$FITC^{hi+}$ and $FITC^-$ $CD11c^+$ DC were isolated from axillary and inguinal lymph nodes, and $FITC^-$ $CD11c^+$ DC were isolated from spleens. For the isolation of lymph node (LN) DC, a patch of dorsal skin from BALB/c mice was shaved and painted with 100 μl of FITC [20 mg $ml^{-1}$ dissolved in acetone:dibutyl phthalate, 1:1, v/v (43)]. Eighteen hours later (time of maximal migration of $CD11c^+$ skin DC to the draining LN; G. Randolph, personal communication), the draining inguinal and axillary LNs were harvested, in addition to the spleen. A single-cell suspension of LN cells was stained with antigen-presenting cell (APC)-conjugated anti-$CD11c^+$ antibody (clone N418, eBioscience, San Diego, CA, USA), washed and FACs-sorted (FACs Aria, Becton Dickenson) into $FITC^{hi+}$/$CD11c^+$ and $FITC^-$/$CD11c^+$ populations (>95% purity was obtained from the sorted populations). For subsequent functional analysis, the sorted cells were counted and plated into 96-well round-bottom plates (Costar) at a concentration of $2.5 \times 10^4$ per well. For flow cytometric analysis of cell surface markers, the sorted cells were immediately stained. Spleen $CD11c^+$ cells were isolated by positive selection using MACS reagents according to the manufacturer's instructions (Miltenyi Biotech, Auburn, CA, USA). The spleen $CD11c^+$ cells were cultured identically as sorted LN $CD11c^+$ in the co-cultured experiments analysis. Spleen $CD11c^+$ DC were FITC negative as assessed by flow cytometry. Naive $CD4^+$ T lymphocytes from DO11.10 TCR transgenic mice were isolated by harvesting the inguinal, mesenteric and axillary LNs and spleen. Naive $CD4^+$ T cells were purified using MACS reagents ($CD4^+$, $CD62L^+$), and >97% purity was routinely achieved as assessed by flow cytometry. For co-culturing with isolated $CD11c^+$ DC, $2.5 \times 10^5$ T cells were added per well together with 4-μM $OVA_{323–339}$ peptide (Peptides International, Louisville, KY, USA). The cells were cultured in DMEM (Mediatech), supplemented with 10% FCS (Lonza Biowhittaker), 2 mM glutamine (Mediatech), 10 mM HEPES (Mediatech), 100 μM non-essential amino acids (Mediatech), sodium pyruvate (Mediatech), 50 μM β-mercaptoethanol, penicillin and streptomycin (Mediatech). There was a minimum of five wells per condition. After 72 h, the supernatants were harvested and assayed for cytokines by ELISA analysis. The cultured cells were analyzed for either FoxP3 (FoxP3 staining kit, according to the manufacturer's instructions, eBioscience) or CTLA4 (clone UC10-489, eBioscience) expression. The mRNA was also isolated from the cultured cells using the Oligotex mRNA isolation kit according to the manufacturer's instructions (Qiagen Sciences) for quantitative PCR (qPCR) analysis. Additionally, in some experiments, the cultures were pulsed with 5-bromo-2-deoxyuridine (BrdU) for the final 12 h and assayed for BrdU incorporation according to the manufacturer's instructions (BD-Pharmingen).

*Flow cytometric analysis*

FACs-sorted $FITC^{hi+}$ and $FITC^-$ $CD11c^+$ DC were prepared and stained for flow cytometry immediately after sorting as previously described (25). Briefly, the cells were incubated for 10 min with Fc block (Becton Dickinson-Pharmingen) to inhibit non-specific binding. The cells were subsequently incubated on ice and stained with anti-mouse OX40L (clone RM134L, eBioscience), anti-mouse MHC class II (clone M5/114.15.2, eBioscience), anti-mouse GITRL (clone eBio YGL 386, eBioscience), anti-mouse CD80 (clone 16.10A1, eBioscience), anti-mouse CD86 (clone GL1, eBioscience), anti-mouse B7RP-1 (clone HK5.3, eBioscience), anti-mouse PD-L1 (clone MIH5, eBioscience), anti-mouse PD-L2 (clone TY25, eBioscience), anti-mouse RANK (clone R12-31, eBioscience) and the appropriate isotype-matched controls. The cells were washed in cold FACS buffer (PBS containing 1% BSA and 0.1% sodium azide) and fixed using BD Cytofix fixation buffer (Becton Dickinson) until analysis using a LSR II analyzer (Becton Dickinson).

## Results

### *Inhibition of CRTH2 ameliorates repeated epicutaneous sensitization-induced inflammation and antigen-specific Ig production*

It has previously been shown that repeated epicutaneous sensitization with the protein antigen chicken egg ovalbumin (OVA) results in the local expression of $T_h2$ cytokines, infiltration of T lymphocytes and eosinophils, as well as OVA-specific antibodies in the serum (19, 21). As numerous cell types involved in this inflammatory process express CRTH2, we investigated the role of the CRTH2 receptor by using a specific small molecule antagonist (Compound A). BALB/c mice were epicutaneously sensitized by securing a patch of gauze saturated with either a 1% OVA/PBS solution or a PBS to a shaved section of back skin, as previously described (19). Separate cohorts of OVA-patched mice received either Compound A or vehicle delivered p.o. or intraperitoneally (i.p.) administered dexamethasone, during the second and third sensitizations. Histological examination reveals acute inflammation and mononuclear cell infiltration in sections from OVA-sensitized skin but not in the PBS control mice (Fig. 1). Strikingly, the OVA/Compound A and OVA/dexamethasone-treated groups showed a strongly reduced inflammatory infiltrate in the dermis, as well as a reduction in the epidermal thickening compared with the OVA/vehicle group.

Analysis of gene expression patterns from the patched skin following the third sensitization period showed an up-regulation of broad spectrum of genes involved in inflammation (Fig. 2A–D). For instance, pro-inflammatory cytokines and chemokines such as tumor necrosis factor (TNF)-α, IFN-γ, IL-1β, IL-24, MIP-1β (CCL4), eotaxin (CCL11), TARC (CCL17), KC (CXCL1) and MIP-2 (CXCL2) are up-regulated in the OVA-treated animals and reduced by Compound A treatment (Fig. 2A). Similarly, CD antigen markers from many of these cell types that respond and/or produce these cytokines and chemokines are reduced, including the CD3 antigen cluster, the DC and Langerhans cell markers CD207 and CD209c and CD14 (Fig. 2B), suggesting a reduced number of these pro-inflammatory cells in the patched skin sections. Importantly, message for CRTH2 (GPR44) and the leukotriene receptors LTB4 receptor 1 and 2 is reduced upon Compound A treatment (Fig. 2C). The mRNA levels of genes linked to inflammatory skin diseases and the atopic phenotype in humans are up-regulated by epicutaneous OVA sensitization and decreased by Compound A, including the calgranulin A and B family members, small proline-rich

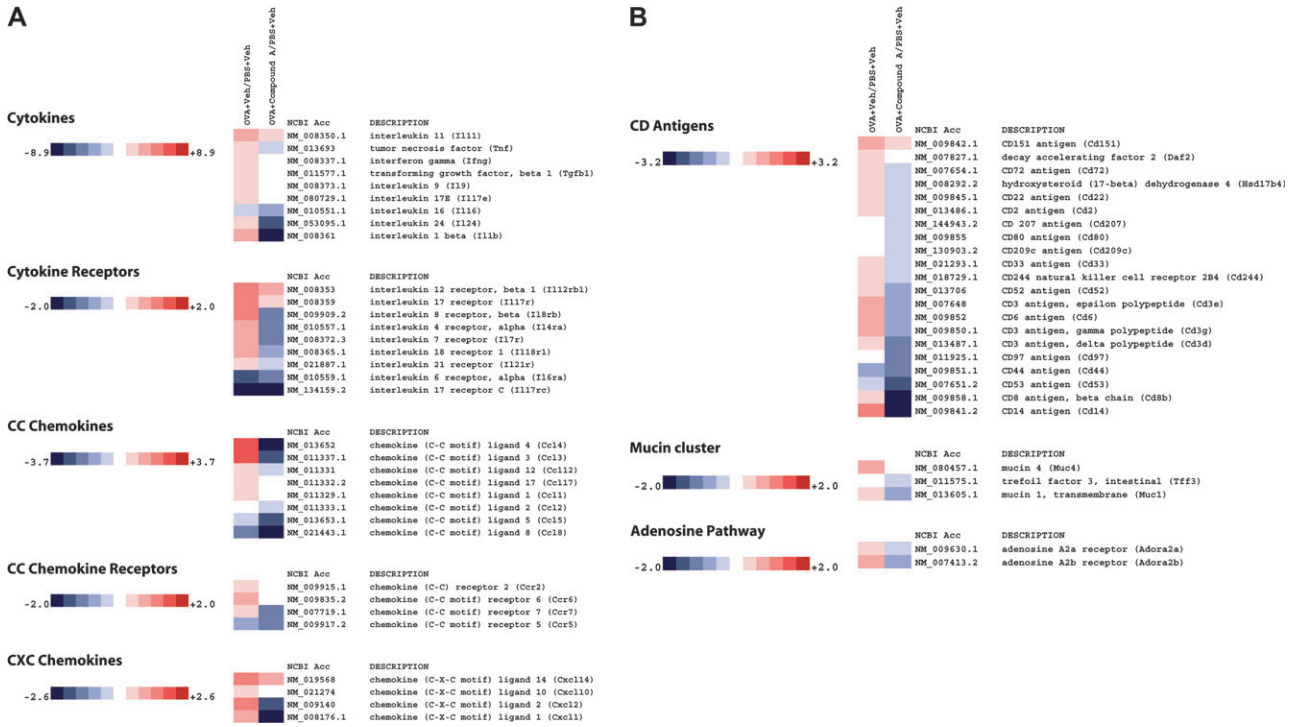


**Fig. 2.** Heatmap of select genes down-regulated in OVA skin patch treated with Compound A. Total RNA was extracted and analyzed using Illumina beadarrays. Levels of gene expression in OVA skin patch ± Compound A were compared with mice treated with just a PBS skin patch. Data are presented as fold increase or decrease in OVA skin patch ± Compound A relative to mice treated with a PBS skin patch. The data array is representative of three independent experiments (biological replicates). The fold changes are noted on the respective color scales. In the clustergrams, genes are grouped into (A) cytokines, cytokine receptors, CC chemokines, CC chemokine receptors and CXC chemokines. (B) CD antigens, mucin cluster and adenosine pathway. (C) Arachidonic acid pathway, signaling molecules and transcription factors. (D) Levels of CD3γ antigen, IL-1β (Il1b), CD14 antigen (Cd14) and calcium-binding protein A9 (calgranulin B) (S100a9) gene expression as determined by RT–qPCR. The data were normalized relative to β-actin and are presented as fold increase or decrease in OVA skin patch ± Compound A relative to mice treated with a PBS skin patch. The RT–qPCR is representative of two independent experiments (biological replicates) performed in duplicate.

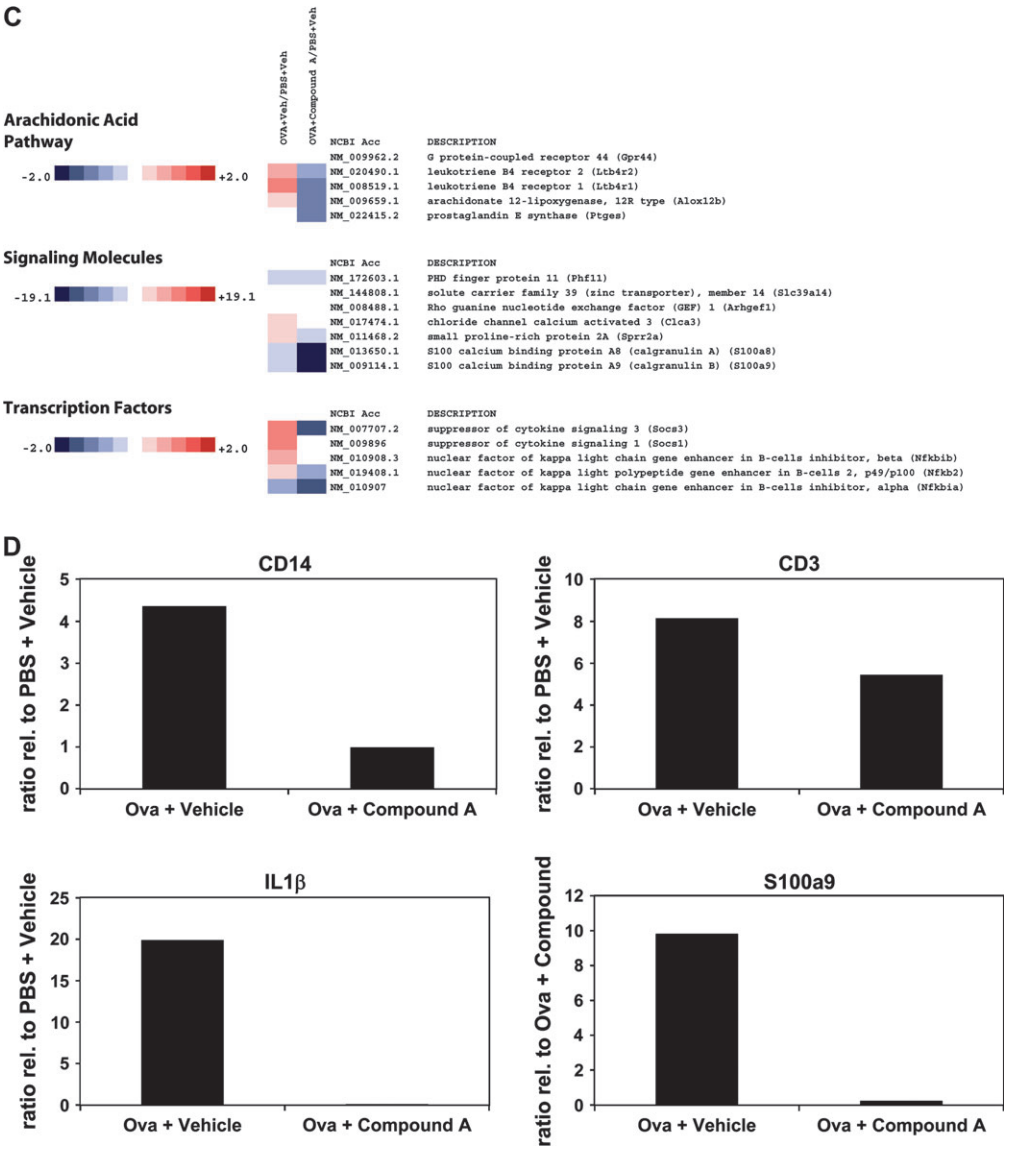


**Fig. 2.** continued.

protein 2A and the IL-4 receptor α-chain (26–29). The qPCR analysis showed an almost complete inhibition of IL-1β RNA induced by OVA treatment (Fig. 2D). Similarly, qPCR analysis of OVA-sensitized skin sections demonstrated that RNA levels of CD14, CD3γ and the atopy-linked gene S100a9 were strongly reduced in mice that received Compound A compared with the drug vehicle-treated animals (Fig. 2D). Finally, it should be noted that the qPCR data on a selection of genes confirm the microarray analysis for the genes examined.

In addition to examining RNA expression patterns from patched skin, protein lysates were also made, and local production of cytokines was examined. In line with the gene expression analysis, both MIP-1β and IL-1β protein levels were elevated in OVA-sensitized skin compared with the PBS control skin sections (Fig. 3). However, the administration of Compound A during the sensitization period significantly reduced the levels of these pro-inflammatory factors. A similar reduction was seen with IL-4, where levels in the OVA-patched skin were almost 3-fold greater than PBS-patched skin, and the administration of either Compound A p.o. or i.p. dexamethasone lowered IL-4 levels to that of PBS controls.

As has been previously reported, epicutaneous sensitization using OVA resulted in increased antigen-specific Ig levels (19). Analysis of serum antibody levels in this study showed a similar increase following three sensitization periods. A dramatic decrease in total IgE levels, as well as OVA-specific IgE, IgG1 and IgG2a was observed in mice treated with Compound A at a dose of 10 mg $kg^{-1}$ (Fig. 4). A significant decrease was also noted in mice treated with just 0.1 mg $kg^{-1}$ of Compound A. As a positive control, dexamethasone delivered via the i.p. route also reduced levels of total and OVA-specific IgE and OVA-specific IgG2a

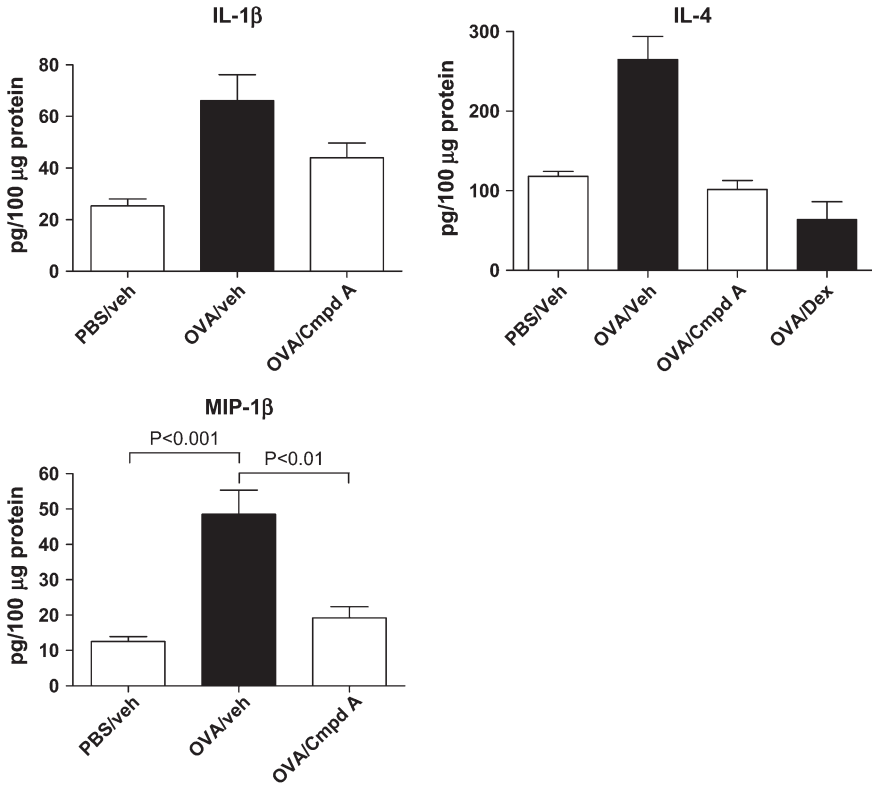


**Fig. 3.** Protein levels of IL-1β, IL-4 and MIP-1β in sensitized skin sections of mice treated with PBS/drug vehicle, OVA/drug vehicle, OVA/Compound A (10 mg $kg^{-1}$) and OVA/Dex (5 mg $kg^{-1}$). A 100 μg of protein from homogenized skin lysates was examined by ELISA. The columns represent the mean ± SEM, $n$ = 5 mice per treatment group.

levels. Interestingly, dexamethasone treatment did not impact the antigen-specific levels of IgG1. Collectively, these results demonstrate that antagonism of the CRTH2 receptor results in a reduction of antigen-specific Igs of multiple classes, as well as local decreases in the production of pro-inflammatory cytokines and chemokines, both at the RNA and protein levels. These decreases may certainly explain the reduced inflammation imparted by Compound A treatment observed histologically in the OVA-sensitized skin. It should also be pointed out that the effect of CRTH2 antagonism by Compound A reduced both $T_h1$ and $T_h2$ cytokines and chemokines, as well as different classes of Igs, not just $T_h2$-associated IgE and IgG1, as has been reported in other studies using CRTH2 gene-deficient mice (12, 30).

### *CRTH2 plays an integral role in regulating inflammation and IgE production in a FITC-induced contact hypersensitivity model*

We next wanted to examine whether antagonism of CRTH2 could influence the contact hypersensitivity response to the antigen FITC. FITC was painted on the abdomen of BALB/c mice on days 1, 2, 14 and 15. On day 25, the mice were challenged by placing FITC on the right ear, and as a control, the FITC vehicle (acetone:dibutyl phthalate) on the left ear. One group of mice received Compound A daily from days 14 to 25, while another received Compound A only on day 25. Twenty-four hours post-ear challenge, the time point of peak edema, the ear thickness was measured and serum was isolated for total IgE antibody quantitation. As can be seen in Fig. 5(A), the administration of Compound A on day 25 dramatically reduced the ear inflammation, and this effect was even greater in mice treated from days 14 to 25. Analysis of total IgE antibody levels showed a significant decrease in the cohort receiving Compound A on days 14 to 25 (Fig. 5B). Thus, in two different models of cutaneous inflammation, antagonism of CRTH2 resulted in decreased inflammation together with reduced antibody production.

### *Blockade of CRTH2 reduced antibody production in response to epicutaneously administered antigens*

As the production of antigen-specific Igs plays a key role in the pathogenesis of allergic disorders such as AD and asthma, we examined in greater depth the ability of the CRTH2 antagonist drug to inhibit antibody production. BALB/c mice received a single-epicutaneous administration of OVA in the same manner as the chronic studies mentioned. A cohort of mice also received Compound A (10 mg $kg^{-1}$) delivered p.o. once a day only during the sensitization period, and serum antibody levels were measured at various time points. Antigen-specific antibodies usually begin to appear in the serum between days 7 and 9 in this model (Stefen Boehme, unpublished results). By day 9, OVA-specific Igs of all classes examined (IgE, IgG1 and IgG2a) were detected in the serum, and there was an ~30% decrease in antigen-specific antibody levels in the Compound A-treated mice (Fig. 6A). Although the epicutaneous sensitization was

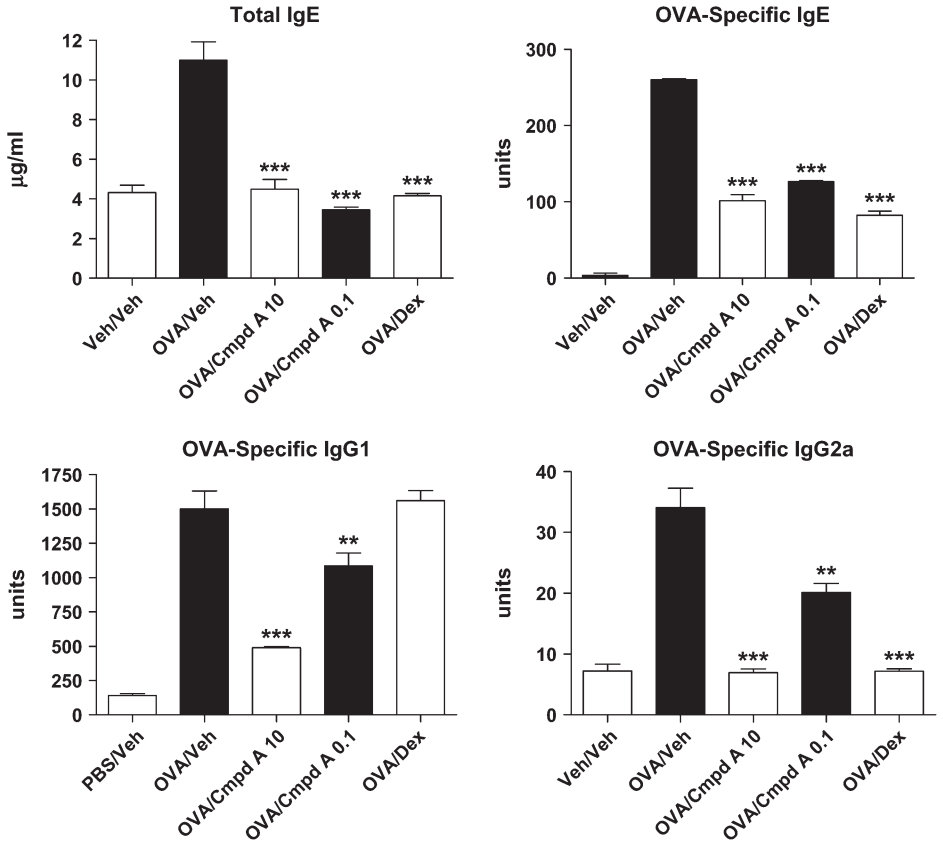


**Fig. 4.** Total IgE and antigen-specific levels of IgE, IgG1 and IgG2a from epicutaneously sensitized mice. Total IgE levels were quantitated by comparison to a standard curve for absolute units, antigen-specific antibody levels are in arbitrary units. Mice were treated with two different concentrations of Compound A: 10 and 0.1 mg $kg^{-1}$ or dexamethasone (5 mg $kg^{-1}$). Each column and error bars display the mean ± SEM. ***$P < 0.001$; **$P < 0.01$. $n = 5$ mice per treatment group, and representative results from two independent experiments are shown.

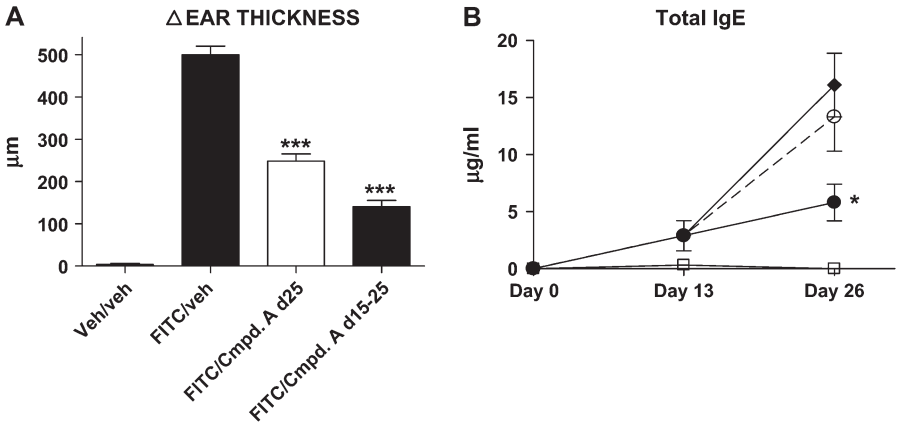


**Fig. 5.** Ear swelling and serum IgE levels from BALB/c mice challenged with FITC. Mice were sensitized to FITC on days 1, 2, 14 and 15 and challenged with FITC on both sides of their right ear on day 25. (A) A 24 h post-FITC challenge, ear thickness was determined by using digital calipers and the Δ (change) in ear thickness was determined by subtracting the width of the right (FITC challenged) ear minus the width of the left (vehicle challenged) ear. Each column shown is the mean ± SEM. (B) Serum was isolated from the mice on days 13 and 26, and the total IgE serum levels were determined. Open squares—vehicle/vehicle-treated cohort, closed diamonds—FITC/vehicle cohort, open circles—FITC/Compound A day 25-treated cohort and closed circles—FITC/Compound A days 14–25-treated cohort. Each point shown is the average ± SEM. ***$P < 0.001$; *$P < 0.05$. A minimum of five mice were used per treatment group, and a representative experiment is shown from four independent experiments.

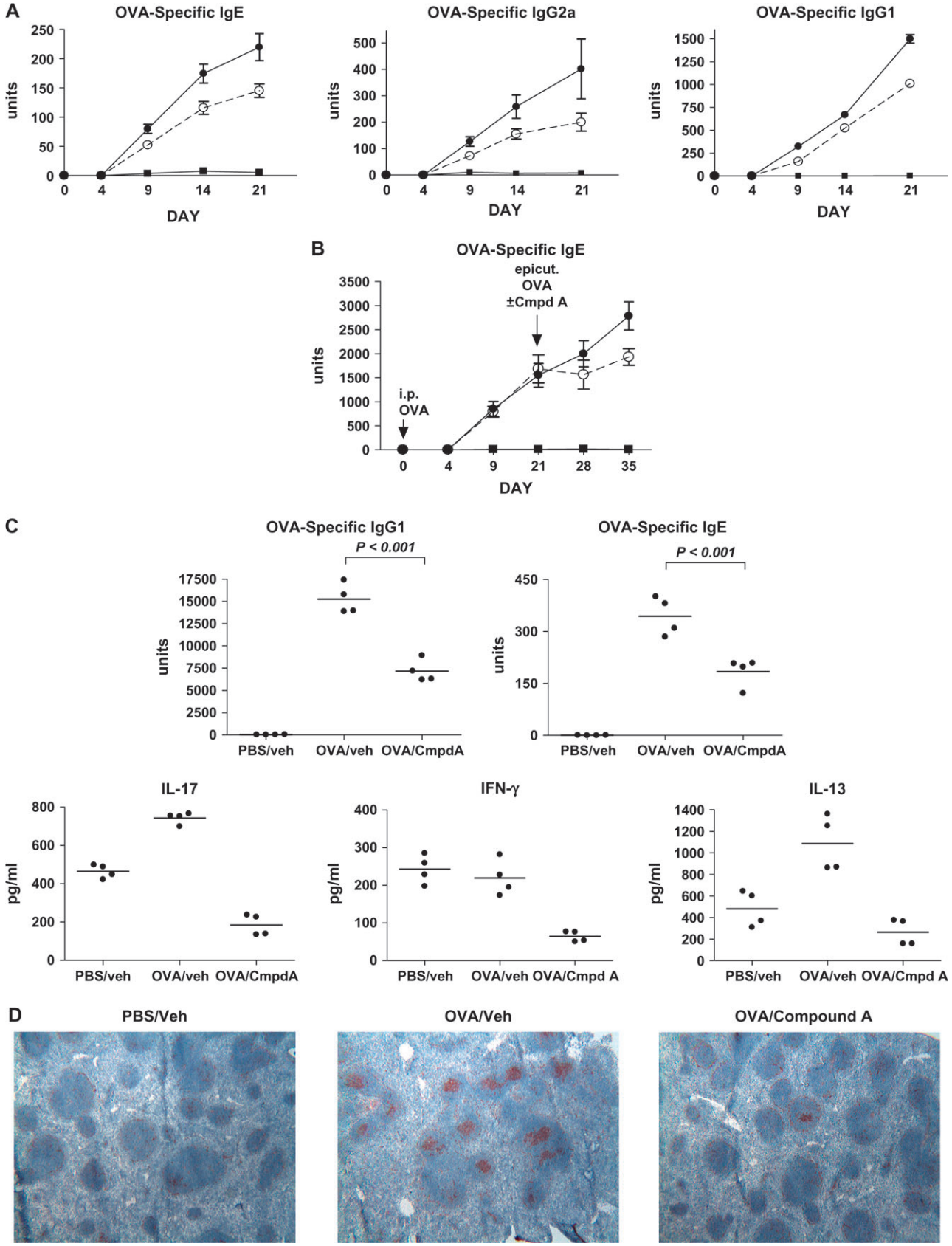
A
OVA-Specific IgE
OVA-Specific IgG2a
OVA-Specific IgG1
units
DAY
B
OVA-Specific IgE
epicut.
OVA
±Cmpd A
i.p.
OVA
units
DAY
C
OVA-Specific IgG1
OVA-Specific IgE
P < 0.001
units
PBS/veh
OVA/veh
OVA/CmpdA
IL-17
IFN-γ
IL-13
pg/ml
OVA/Cmpd A
D
PBS/Veh
OVA/Veh
OVA/Compound A

stopped on day 7 of the experiment, OVA-specific antibody levels continued to rise through day 21. The administration of Compound A also ceased on day 7, yet similar to the day 9 observations, antagonism of CRTH2 consistently resulted in reduced OVA-
specific antibody titers. This effect of Compound A was only observed in response to epicutaneous sensitization, as immunization of OVA protein or OVA-trinitrophenol suspended in the adjuvant alum and administered i.p. was not impacted by Compound A (Fig. 6B, and data not shown). However, when the OVA/alum-immunized mice were subsequently epicutaneously sensitized to OVA for a 7-day period 21 days following the i.p. immunization, the co-administration of Compound A only during the sensitization period caused a marked reduction of OVA-specific antibody levels (Fig. 6B). These observations again suggest that the CRTH2/$PGD_2$ interaction is critical for mounting an optimum antibody response following exposure to cutaneous antigens.

To examine this further, mice, epicutaneously sensitized on days 1–7 with or without Compound A treatment on those days, were sacrificed on day 24, and the splenocytes were cultured with OVA for 72 h. The *in vitro* culture did not contain any Compound A or exogenous $PGD_2$. Analysis of cytokine levels in the culture supernatants showed a striking decrease in IL-13, IL-17A and IFN-γ levels in the cultured splenocytes from Compound A-treated mice (Fig. 6C). This suppressive effect is long lasting, as splenocytes were isolated and re-challenged with antigen *in vitro* 17 days following the last dose of Compound A. Consistent with this, PNA staining of spleen sections from these mice showed that many lymphoid follicles from the OVA/vehicle-treated mice contained many areas of $PNA^+$ cells, presumably activated B cells. In contrast, there was a significant decrease of $PNA^+$ cells in the spleens from the OVA/Compound A-treated mice and, as expected, the PBS/vehicle-treated mice (Fig. 6D). Taken together, these results suggest that the decreased antibody levels observed in Compound A-treated mice following epicutaneous sensitization may be due at least in part to decreased production of cytokines in the secondary lymphoid organs, such as the spleen. The reduction of IL-17A and IFN-γ demonstrates that this effect is not limited to $T_h2$ responses. This decrease in cytokine production, together with the observation that antagonism of CRTH2 decreases antibody production following epicutaneous sensitization, but not i.p. alum immunization, suggests that this effect may be attributed to the ability of skin-derived DC to migrate and present antigen to T lymphocytes in the dLN.

*Skin-derived $CD11c^+$ DC from Compound A-treated mice are less effective at stimulating naive T lymphocytes*

In an effort to understand how antagonism of CRTH2 can modulate DC-mediated T cell activation, we examined activated skin-derived $CD11c^+$ DC for their ability to stimulate naive T cells. BALB/c mice were painted on a shaved section of dorsal skin with FITC, as well as receiving either Compound A or vehicle concomitantly. Eighteen hours later, the dLNs were isolated, and both $FITC^{hi+}$ and $FITC^-$ $CD11c^+$ DC were isolated by Facsorting. Notably, the Compound A-treated mice had lower percentage of $FITC^{hi+}$ DC comprising the total $CD11c^+$ population than vehicle-treated mice (43.2% veh Tx versus 34.7% Cmpd A Tx, Fig. 7). This suggests a decreased migration of $CD11c^+$ skin-derived DC to the dLNs at 18 h post-FITC painting.

The various populations of DC were co-cultured with a 10-fold excess of naive $CD4^+$ T lymphocytes isolated from DO11.10 TCR transgenic mice and the $OVA_{323–339}$ peptide. As a control, splenic $CD11c^+$ DC were isolated from the two groups of FITC-painted mice (e.g. vehicle-treated and Compound A-treated mice) and co-cultured with T cells and antigen. After 72 h, the culture supernatants were harvested and assayed for various cytokines. As shown in Fig. 8, $FITC^{hi+}$ DC from Compound A-treated mice were generally much less effective at eliciting cytokine production from naive T cells than $FITC^{hi+}$ DC from vehicle-treated mice. In particular, production of IL-17A, IFN-γ, IL-10 and IL-6 were substantially decreased in cultures containing $FITC^{hi+}$ DC from Compound A-treated mice. For instance, IL-17A levels were reduced to ~50%, and there was a 40% decrease in the amount of IFN-γ produced, and this decrease was readily detectable after 48 h in culture (Fig. 8). Levels of IL-4, although low in all conditions tested, were not significantly altered among the different DC populations. Similarly, the levels of transforming growth factor (TGF)-β1 and IL-27, a negative regulator of $T_h17$ differentiation, were not impacted between the different DC populations (data not shown). An examination of cytokines that could be produced by the DC directly revealed that no IL-12, IL-6 or IL-10 was detected in the supernatants from any of the DC populations cultured in the absence of T cells and antigen. The possibility does remain, however, that DC could have been induced to produce the IL-6 and IL-10 upon culture with the naive T cells and antigen, as opposed to this being exclusively T cell-mediated cytokine production. Using qPCR, no significant differences in the RNA levels of IL-23/p19 were

**Fig. 6.** CRTH2 antagonism results in reduced serum levels of OVA-specific antibodies in epicutaneously ovalbumin-sensitized BALB/c mice. (A) Mice were sensitized epicutaneously on days 1–7, with either PBS or OVA, and dosed daily with either drug vehicle or compound A (10 mg $kg^{-1}$) for the same time period. Serum was isolated on days 4, 9, 14 and 21 and assayed for OVA-specific IgE, IgG1 and IgG2a. Closed squares—PBS/vehicle cohort ($n$ = 6), closed circles—OVA/vehicle cohort ($n$ = 12) and open circles—OVA/Compound A cohort ($n$ = 12). Each point shown is the mean ± SEM. (B) Mice were i.p. immunized with 10 μg OVA dissolved in alum or alum alone on day 1. On day 21, the mice receiving the OVA/alum were epicutaneously sensitized with OVA for 7 days, and one cohort received Compound A (10 mg $kg^{-1}$) for days 21–27. Serum was isolated on days 4, 9, 21, 28 and 35 and OVA-specific IgE antibodies were measured. The three groups were as follows: closed squares—alum alone and PBS epicutaneously immunized ($n$ = 5), closed circles—OVA/vehicle cohort ($n$ = 10) and open circles—OVA/Compound A cohort ($n$ = 10). Each point shown is the mean ± SEM. (C) Mice were epicutaneously sensitized to PBS or OVA and dosed with either drug vehicle or Compound A on days 1–7. After removing the skin patches on day 7, the mice were left unmanipulated until day 24, at which time the spleen was isolated and serum was drawn. OVA-specific IgE and IgG1 serum levels were determined. The spleen cells were cultured at $2 \times 10^6$ splenocytes per well of a 96-well round-bottom plate in the presence of 1 μg $ml^{-1}$ OVA for 72 h. Supernatants were harvested and analyzed by ELISA for IL-17A, IL-13 and IFN-γ. The value from each individual mouse is shown, and the horizontal bars represent the median. (D) Spleen sections from mice treated as in (C) were stained with PNA to show areas of activated B lymphocytes in the lymphoid follicles.

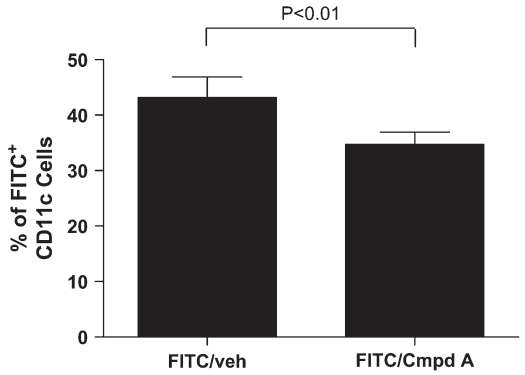


**Fig. 7.** Compound A-treated mice had a decreased number of FITC$^{hi+}$ CD11c$^{+}$ DC than FITC-painted vehicle-treated mice. A 18 h post-administration of a 2% FITC solution to shaved dorsal skin of BALB/c mice and oral dosing of Compound A (10 mg kg$^{-1}$) or drug vehicle, the inguinal and axillary dLNs were harvested, and the cells stained for CD11c. The lymph node cells were then FACS sorted for CD11c$^{+}$/FITC$^{hi+}$ cells and CD11c$^{+}$/FITC$^{-}$ cells. The total number of FITC$^{hi+}$ CD11c$^{+}$ cells versus the total number of CD11c$^{+}$ cells was used to calculate the percentage of FITC$^{hi+}$ cells from the total CD11c$^{+}$ cells for each treatment group (FITC/vehicle versus FITC/Compound A). The results are from five separate experiments, and the *P* value is <0.01.

detected between the different DC populations (data not shown). As IL-6 and TGF-β are important for the induction of IL-17A expression and IL-23 is necessary for the expansion of $T_h17$ cells, these data suggest that the differences in IL-17 production by the DO11.10 T cells co-cultured with different populations of CD11c$^{+}$ DC cannot be attributed to these cytokines.

Intracellular staining analysis following the 72 h co-culture revealed no significant differences in the percentage of FoxP3$^{+}$ or CTLA-4$^{+}$ T cells between the various DC/T cell cultures (data not shown). This coupled with the observation that FITC$^{hi+}$ DC from Compound A-treated mice had reduced levels of IL-10 suggest that induction of a Treg population was not the cause of the cytokine suppression. Analysis of various cell surface molecules expressed by the FITC$^{hi+}$ CD11c$^{+}$ DC from either the Compound A or vehicle-treated mice revealed no significant differences. More specifically, the expression levels of MHC class II, CCR7, RANK ligand, the co-stimulatory ligands B7-1, B7-2, ICOS ligand, OX-40 ligand, CD40 and negative co-stimulatory molecules GITR ligand, PD-L1 (Fig. 9) and PD-L2 were similar between the two groups of FITC$^{hi+}$ CD11c$^{+}$ DC (Fig. 9, data not shown). However, cell surface levels of all these molecules were up-regulated in the FITC$^{hi+}$ CD11c$^{+}$ DC compared with the FITC$^{-}$ CD11c$^{+}$ DC isolated (Fig. 9, data not shown).

In summary, the administration of Compound A reduced the number of activated, skin-derived FITC$^{hi+}$ CD11c$^{+}$ DC in the dLN. Further, when equal numbers of DC isolated from either vehicle-treated or Compound A-treated mice are cultured with naive CD4$^{+}$ T cells, there is a marked reduction in a number of pro-inflammatory T cell cytokines produced. This reduction in cytokine production coupled with a decreased amount of migrating, activated skin DC may account for the decrease in specific Igs observed. This, in turn, may explain, at least in part, the decreased cutaneous inflammatory response seen with Compound A-treated mice in two models of allergic dermatitis.

## Discussion

AD is a common inflammatory skin disease with lesions characterized by epidermal thickening and a prominent perivascular and dermal infiltrate, as well as high serum IgE levels. In this study, we used two well-characterized murine models of AD to examine the role of CRTH2 in cutaneous inflammation. Both of these models are CD4$^{+}$ T lymphocyte dependent, as is AD (16, 19, 31). In a model of repeated epicutaneous sensitization, the administration of a CRTH2 antagonist reduced inflammation in the dermis substantially, as well as prevented epidermal thickening (Fig. 1). Using a robust 25 day FITC model of contact hypersensitivity, the administration of the CRTH2 antagonist just prior to challenge substantially blocked ear swelling (~50% decrease). Additionally, administration of Compound A from days 14 to 25 inhibited inflammation further still, reducing ear thickness ~75% compared with untreated controls (Fig. 5A). Importantly, an examination of serum Ig levels showed a decrease in total IgE in animals treated with the CRTH2 antagonist in both *in vivo* models (Figs 4 and 5B). Further, in the epicutaneous OVA sensitization model, where antigen-specific antibody levels could reliably be measured, there was a decrease in OVA-specific IgE, IgG1 and IgG2a levels. A closer examination of this was carried by epicutaneously sensitizing mice to OVA for a 1-week period while administering drug vehicle or Compound A. Again, an antigen-specific decrease was seen in the IgE, IgG1 and IgG2a Ig classes upon administration of the CRTH2 antagonist (Fig. 6A). As antibody titers to protein antigens rise substantially with repeated immunizations, the effect of Compound A became more pronounced. Hence, we observed a much greater effect on Ig levels in the chronic OVA model, with Compound A administered during the second and third patching (Fig. 4) than after the first patching (Fig. 6A). It should also be pointed out that antibody production was not affected by the CRTH2 antagonist following intra-peritoneal immunization with same protein antigen, ovalbumin, emulsified in the adjuvant alum. This suggests that the route of antigen delivery and subsequent presentation may play a key role in determining the influence of a CRTH2 blockade. These findings confirm and extend the findings of Nakamura *et al.* using a CRTH2$^{-/-}$ mice bred to the BALB/c background (12, 30). They initially reported a modest decrease in total IgE levels in CRTH2$^{-/-}$ mice following multiple cutaneous sensitizations with TNCB (12). This slight decrease may be attributable to the fact that this model is not T cell dependent (32). In a novel model of allergic rhinitis, intranasally sensitized CRTH2-deficient mice had a reduction in antigen-specific IgE and IgG1 (30). However, in this model, very low levels of antigen-specific IgG2a were detected in the serum, in contrast to this report and studies by Geha *et al.* using epicutaneous sensitization with ovalbumin (19, 30). These different results with respect to IgG2a may be due to different modes of antigen sensitization or the antigen itself (ovalbumin or Cry j 1 antigen). Taken together, however, these findings are of great importance given the role allergen-specific

antibodies play in allergic inflammation diseases, such as AD, allergic rhinitis and asthma. This also implied that CRTH2 was not only having an effect on both acute inflammation (administration of Compound A at the time of FITC challenge; Stefen A. Boehme, unpublished results) but also having an effect on the underlying immune response resulting in antibody production to epicutaneously administered antigen.

Examination of gene expression levels from skin that had been epicutaneously sensitized to ovalbumin showed a robust pattern of gene up-regulation across the mouse genome (Fig. 2A–C). In line with epicutaneous OVA sensitization generating a predominantly $T_h2$-type T cell response, a wide array of cytokines, chemokines and their cognate receptors and associated signaling molecules were found to be dramatically up-regulated. Much attention has been focused on the chemokine superfamily as the major stimulus for the directed migration of leukocytes during the elicitation phase of hypersensitivity reactions in skin. Additionally, much discussion has centered on the segregation of such mediators into their ability to promote $T_h1$-type or $T_h2$-type responses. While a large number of cytokines and chemokines were up-regulated, members of the MCP family of chemokines (CCL2/MCP-1, CCL8/MCP-2, CCL12/MCP-5) as well as CCL1/I-309, CCL3/MIP-1α, CCL4/MIP1β and the CXCL family members CXCL1/GRO-α and CXCL2/GRO-β, CXCL10/IP-10 and CXCL14/BRAK appeared to be the most relevant (Fig. 2A). It is clear from this group of chemokines that there is no distinction of the $T_h1$- or $T_h2$-type responses since a wide array of cells including B cells, macrophages and neutrophils are stimulated by these chemokines. Studies in a different model of epidermal inflammation have shown that the CXCR2 ligands GRO-α, the murine ortholog of IL-8 and MIP-2, can induce a significant inflammatory state (33). Both GRO-α and MIP-2 are up-regulated in our model and Compound A treatment significantly down-regulated the gene expression (Fig. 2A). The gene for IP-10 was also noted to be up-regulated by OVA challenge and was significantly down-regulated by Compound A (34). A number of T lymphocyte cell surface molecules, such as CD3ε, γ and δ, increase after OVA skin patching, but are strongly reduced by Compound A treatment (Fig. 2B and D). As the inflammatory infiltrate into the dermis is primarily made up of T lymphocytes, both in this model and AD, the decrease in T cell gene expression is consistent with reduced inflammation (16, 19), and this may have important therapeutic implications.

Further investigations of the profiles of gene regulation have revealed interesting correlations with findings from assessment of the genetic risk factors associated with human atopy—specifically AD and asthma, two of the primary constituents of the 'atopic march' (26). A large number of population studies have been conducted to elucidate genetic risk factors for atopy and its disease manifestations in different organs. With regard to AD in humans, several loci have been revealed including those encoding genes in the so-called epithelial differentiation complex (SPINK5, SPRR and S100A gene families) (35–37). Our OVA challenge model reveals that Compound A treatment significantly down-regulated the SPRR2a, S100A8 and S100A9 (calgranulin) family members' expression, a finding which may be relevant to the anti-inflammatory efficacy of the CRTH2-specific antagonism (Fig. 2C and D).

Additional genes of interest in the atopy risk loci include the $T_h2$ cytokines/receptors IL-13, TNF-α, IL-9, IL-17E, IL-18, IL-4 receptor α and the chemokine eotaxin (CCL11). In our hands, the cytokines TNF-α, IL-9, IL-17E as well as the receptors IL-4 receptor α and IL-18 receptor were shown to be up-regulated by OVA sensitization and significantly affected by Compound A treatment. Other miscellaneous risk factors include the proteases diprolylpeptidase 10, A disintegrin and metalloprotease family member 33 (ADAM33), the plant homeodomain finger protein 11 (PHF11) and the solute carriers SLC9A3R1 and SLC22 families. While a number of these factors are more relevant to the asthma phenotype, we have certainly noted an up-regulation in several of the SLC family members (data not shown). In the OVA-challenge model described here, expression of the monocyte CD antigen, CD14, increased, and Compound A treatment significantly down-regulated CD14 gene expression (Fig. 2B and D). Similar findings have been shown for the dendritic and Langerhan's cell markers CD207 and CD209c. Finally, in the treated skin sections, protein levels of IL-1β, IL-4 and MIP-1β (CCL4) were reduced by Compound A, a result consistent with the gene expression data. Taken together, this data suggested that the CRTH2 antagonist has a greater effect than just inhibiting the infiltration of $CRTH2^+$ cells, but appears to act on a variety of genes involved in many aspects of the allergic inflammatory response.

An examination of cytokines produced by splenocytes from epicutaneously OVA-sensitized mice, 17 days after the initial OVA sensitization period and Compound A treatment period, showed a decrease in the IL-13, IFN-γ and IL-17A levels. The effect on IFN-γ and IL-17A suggests that Compound A is exerting an effect on more than just classical $T_h2$ cells. Perhaps, this could be explained by the observation that murine $T_h1$ cells also express CRTH2. Alternatively, expression patterns of CRTH2 show its expression in many unexpected tissues (7). In the human system, we have observed that atopic and/or asthmatic patients express CRTH2 on numerous other leukocytes besides $CCR4^+$ $CLA^+$ $T_h2$ T lymphocytes (Stefen A. Boehme, unpublished results). Finally, it is possible that antagonism of CRTH2 may be exerting an indirect effect on $T_h$ cell subsets besides $T_h2$ cells. Nonetheless, these observations demonstrate that the administration of the CRTH2 antagonist *in vivo* appears to have a broad effect on the immune response to antigens delivered epicutaneously, and this effect extended significantly past the bioavailability of Compound A. Further, the observation that blockade of CRTH2 can impact cytokine production in multiple types of $T_h$ cells, including $T_h1$, $T_h2$ and $T_h17$ cells is novel, as this has not been fully explored in studies using CRTH2 gene-deficient mice (12, 13, 30).

As epicutaneous antigen sensitization is thought to be critical for AD and to account for the effect of the CRTH2 antagonist on epicutaneously immunized antigen, we hypothesized that skin DC may play a role. Both dermal DC and Langerhans cells are able to take up antigen in the skin, migrate to the dLNs and initiate T cell-mediated immune responses (38). Therefore, we examined the role that professional dermal APCs may play in shaping an immune response. After FITC

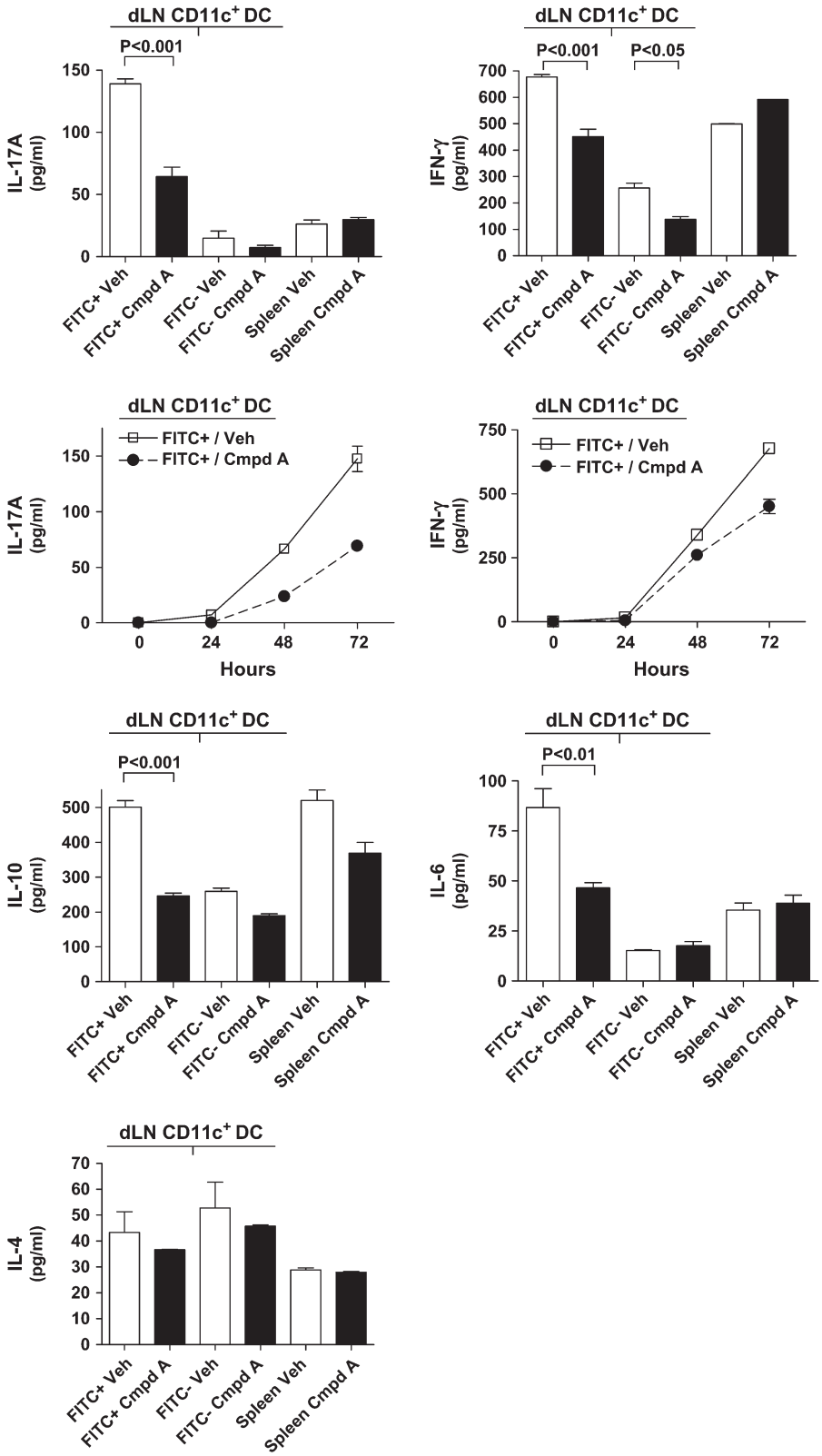


**Fig. 8.** CD11c$^+$ DC have different capacities to stimulate cytokine production by naive CD4$^+$ TCR transgenic T cells. Mice were treated with Compound A or drug vehicle together with FITC administration to the dorsal skin. After 18 h, the draining LNs and spleens were harvested. Both dLN FITC$^{hi+}$ and FITC$^-$ CD11c$^+$ populations were isolated by FACS sorting, and splenic CD11c$^+$ cells were harvested by MACS separation. After the different CD11c$^+$ DC populations were isolated, the cells were cultured with a 10-fold excess of CD4$^+$ naive T cells from DO11.10 TCR transgenic mice and 4-μM OVA$_{323–339}$ peptide. After 24 and 48 h, an aliquot of the culture supernatant was removed, and the remaining culture

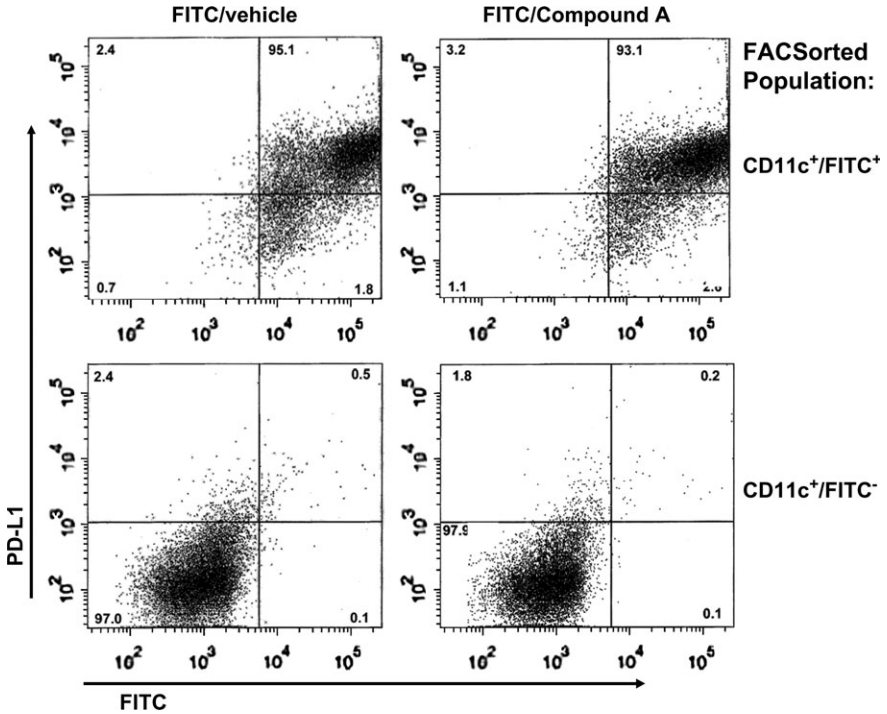


**Fig. 9.** Flow cytometric analysis of PDL-1 levels on CD11c$^+$ DC isolated from FITC-painted mice that received either Compound A or drug vehicle. The FITC$^{hi+}$ and FITC$^-$ CD11c$^+$ populations derived from the dLNs were isolated by FACS sorting. The percentage of each cell phenotype is listed in the respective quadrant. Approximately 5% of the FITC$^{hi+}$ cells became FITC$^{lo+}$ compared with the cell-sorted populations immediately after sorting. These DC apparently lost FITC taken up during the FACs staining step or fixation in PFA. A representative experiment from an $n = 2$ is shown.

was applied to dorsal skin, as opposed to OVA–FITC which gave a very weak response similar to observations of other groups (20), we detected a slight but significant decrease in the number of FITC$^{hi+}$ CD11c$^+$ DC that migrated from the skin to the dLN in Compound A-treated mice. This difference was not detected in earlier studies using CRTH2$^{-/-}$ mice, as the percentage of FITC$^+$ cells was compared with whole lymph node cell population, as opposed to just the CD11c$^+$ cells (12). Further, our results show that a high percentage of the FITC$^{hi+}$ cells in the dLN express CD11c, strongly suggesting that these cells migrated from the skin, as opposed to acquiring FITC via the lymph or blood stream. Co-culturing of the different populations of CD11c$^+$ DC, those expressing high levels of FITC, the resident CD11c$^+$ DC in the lymph nodes that were FITC$^-$ and splenic-derived CD11c$^+$ DC, showed striking effects on their ability to activate naive T cells. As noted previously, FITC$^{hi+}$ CD11c$^+$ DC elicited a much greater IL-17A response compared with splenic-derived CD11c$^+$ DC co-cultured with naive T cells (Fig. 8; 20). However, the FITC$^{hi+}$ CD11c$^+$ DC isolated from Compound A-treated mice elicited substantially decreased levels of IL-17A, IFN-γ, IL-10 and IL-6 upon co-culture with naive DO11.10 TCR transgenic T cells compared with vehicle-treated animals. As IL-6 has been shown to play a role in the differentiation of $T_h17$ cells, perhaps this decrease in IL-17A may be linked to the decrease of IL-6 produced by naive T cells co-cultured with FITC$^{hi+}$ CD11c$^+$ DC from Compound A-treated mice (39, 40). However, this decrease is already detected in cultures after 24 h and the CD11c$^+$ cells do not make any IL-6 when cultured in the absence of T cells or antigen (Fig. 4). Additionally, no significant differences in the amount of TGF-β cytokine or IL-23 mRNA levels were detected between the various DC populations.

This decreased amount of cytokine production does not appear to be mediated by the induction of a regulatory T cell population, as we found no increase of FoxP3$^+$ cells, or CTLA-4$^+$ cells in the cultures after 72 h (data not shown). The levels of IL-10 were not increased in the cultures containing the FITC$^{hi+}$ CD11c$^+$ DC from Compound A-treated mice. IL-6 was present in the same cultures and if a Treg population was induced, IL-6 levels would be expected to be greatly decreased. The FITC$^{hi+}$ DC derived from Compound A-treated mice did not appear to induce anergy in the naive T cell population, as the levels of IL-4 produced were not significantly different among the different DC

supernatant (200 μl) was removed at 72 h. The culture supernatants were assayed by ELISA for IL-17A, IFN-γ, IL-10, IL-6 and IL-4 levels, and additionally the IL-17A and IFN-γ levels were determined for the 24 and 48 h-time points. The results from the co-cultures containing the dLN CD11c$^+$ DC are labeled dLN CD11c$^+$ DC. Each bar graph shows a representative experiment of a minimum of three independent experiments. Each column represents the mean cytokine value obtained from that experiment ± SEM. For the kinetic analysis of IL-17A and IFN-γ, each point represents the average value ± SEM and results of a representative experiment of $n = 2$ are shown.

populations examined (Fig. 8). Further, the percentage of cells in the S or $G_2$/M phase of the cycle, or $BrdU^+$, was not significantly changed between the different DC groups tested (data not shown). Finally, the levels of various cell surface proteins expressed by DC involved in T cell activation were very similar between the $FITC^{hi+}$ $CD11c^+$ DC from both the Compound A-treated or untreated mice (Fig. 9). Collectively, this indicates that the Compound A-derived DC can process and present antigen efficiently to T cells. Additionally, various activation molecules were greatly increased, as expected, by the skin emigrant $FITC^{hi+}$ DC in the draining LN compared with resident DC (Fig. 9).

Thus, the mechanism by which DC, that migrated from the skin to the draining LN upon antigen capture from the CRTH2-antagonized mice, are able to suppress cytokine production when used to stimulate naive T cells is still unclear. Possible insight into a mechanism comes from our studies using a 1-week FITC-induced contact hypersensitivity model, which demonstrated that antagonism of CRTH2 led to a substantial decrease in TSLP and IL-1β protein levels (Boehme, S.A., Franz-Bacon, K., Chen, E.P., Šášik, R., Sprague, L.J., Ly, T.W., Hardiman, G and Bacon, K.B., submitted for publication). This decrease would be expected to have a profound effect on both skin DC and Langerhans cells as TSLP has been shown to trigger both activation and migration of these skin DC populations (41, 42). Consistent with this notion, we observed in our gene expression studies of epicutaneously sensitized skin, a decrease in CCL17/TARC mRNA levels upon Compound A treatment (Fig. 2A). TSLP activation of DC has been shown to stimulate TARC production (41). Taking this a step further, the effect of activated skin DC from Compound A-treated mice to suppress cytokine production in this *in vitro* culture model appears to reproduce the *in vivo* effect, as (1) spleen cells from epicutaneously immunized and Compound A-treated mice also showed a marked decrease in cytokine production upon antigen re-stimulation (Fig. 6C). And (2) there is a profound decrease in various cytokine and chemokines mRNAs imparted by Compound A treatment of epicutaneously sensitized mice to OVA (Fig. 2A). Additionally, the effect on both IFN-γ ($T_h1$) and IL-13 ($T_h2$) cytokines is consistent with a decrease in Ig levels of multiple classes. Taken together, ability of the CRTH2 antagonist to inhibit both cytokine and antibody levels induced by epicutaneous administration of antigen may very well account for the profound effect on the level of inflammation incurred by either repeated epicutaneous OVA-antigen sensitization or multiple FITC sensitizations and challenge. This could certainly cause the decreased inflammatory infiltrate and reduced gene and protein expression of pro-inflammatory mediators observed. These results also strongly suggest that inhibition of CRTH2 would have a greater effect on alleviating allergic inflammation than antagonism of the DP1 $PGD_2$ receptor. Further, Satoh *et al.* (12) report preliminary findings using the $CRTH2^{-/-}$ mice that are consistent with our findings using a CRTH2 antagonist (22). In two different models of murine allergic airway disease, the inflammatory infiltrate and pro-inflammatory cytokine and chemokine production are greatly reduced by deletion or antagonism of CRTH2. These findings are in sharp contrast to the results reported by Chevalier *et al.* (13). Therefore, as Chevalier's results point out, gene KO studies need to be evaluated with the possibility of influence from gene compensatory mechanisms. It may also be possible, though unlikely given Compound A specificity, that the effects we observed could be triggered by mechanisms independent of the $PGD_2$/CRTH2 pathway. We believe this unlikely, however, given the generally complementary results observed here and Nakamura *et al.* using the CRTH2 knockout mice in comparable experiments.

In summary, the ability of potent and specific CRTH2 antagonist compound to decrease cutaneous inflammation and antigen-specific Ig levels strongly suggest that CRTH2 blockade may be powerful therapeutic course for the treatment of AD as well as for allergic rhinitis and asthma.

## Funding

National Institutes of Health/NIDDK to G.H. (1 P30 DK063491-03).

## Acknowledgements

We thank J. Lapira at the UCSD BIOGEM laboratory for Illumina Beadarray processing and quantitative RT–PCR analysis and I. Wick for help with the preparation of figures.

## Disclosure

S.A.B., E.C., T.W.L. and K.B.B. are Actimis Pharmaceuticals shareholders. All other authors have no conflicting interests.

## Abbreviations

| | |
|---|---|
| AD | atopic dermatitis |
| APC | antigen-presenting cell |
| BrdU | 5-bromo-2-deoxyuridine |
| CLA | cutaneous lymphocyte-associated antigen |
| CRTH2 | chemoattractant receptor homologous molecule expressed on $T_h2$ cells |
| DC | dendritic cells |
| dLN | draining lymph node |
| DK-$PGD_2$ | 13,14-dihydro-15-keto-prostaglandin $D_2$ |
| i.p. | intra-peritoneally |
| LN | lymph node |
| OVA | chick egg ovalbumin |
| $PGD_2$ | prostaglandin $D_2$ |
| PNA | peanut agglutinin |
| p.o. | orally |
| qPCR | quantitative PCR |
| TGF | transforming growth factor |
| TNF | tumor necrosis factor |

## References

1 Murray, J. J., Tonnel, A. B., Brash, A. R. *et al.* 1986. Release of prostaglandin D2 into human airways during acute antigen challenge. *N. Engl. J. Med.* 315:800.
2 Miadonna, A., Tedeschi, A., Brasca, C., Folco, G., Sala, A. and Murphy, R. C. 1990. Mediator release after endobronchial antigen challenge in patients with respiratory allergy. *J. Allergy Clin. Immunol.* 85:906.
3 Fujitani, Y., Kanaoka, Y., Aritake, K., Uodome, N., Okazaki-Hatake, K. and Urade, Y. 2002. Pronounced eosinophilic lung inflammation and Th2 cytokine release in human lipocalin-type prostaglandin D synthase transgenic mice. *J. Immunol.* 168:443.
4 Nagata, K., Tanaka, K., Ogawa, K. *et al.* 1999. Selective expression of a novel surface molecule by human Th2 cells *in vivo*. *J. Immunol* 162:1278.
5 Hirai, H., Tanaka, K., Yoshie, O. *et al.* 2001. Prostaglandin D2 selectively induces chemotaxis in T helper type 2 cells, eosinophils,

and basophils via seven-transmembrane receptor CRTH2. *J. Exp. Med.* 193:255.
6 Monneret, G., Gravel, S., Diamond, M., Rokach, J. and Powell, W. S. 2001. Prostaglandin D2 is a potent chemoattractant for human eosinophils that acts via a novel DP receptor. *Blood* 98:1942.
7 Shichijo, M., Sugimoto, H., Nagao, K. *et al.* 2003. Chemoattractant receptor-homologous molecule expressed on Th2 cells activation *in vivo* increases blood leukocyte counts and its blockade abrogates 13,14-dihydro-15-keto-prostaglandin D2-induced eosinophilia in rats. *J. Pharmacol. Exp. Ther.* 307:518.
8 Tanaka, K., Hirai, H., Takano, S., Nakamura, M. and Nagata, K. 2004. Effects of prostaglandin D2 on helper T cell functions. *Biochem. Biophys. Res. Commun.* 316:1009.
9 Xue, L., Gyles, S. L., Wettey, F. R. *et al.* 2005. Prostaglandin D2 causes preferential induction of proinflammatory Th2 cytokine production through an action on chemoattractant receptor-like molecule expressed on Th2 cells. *J. Immunol.* 175:6531.
10 Spik, I., Brénuchon, C., Angéli, V. *et al.* 2005. Activation of the prostaglandin D2 receptor DP2/CRTH2 increases allergic inflammation in mouse. *J. Immunol.* 174:3703.
11 Gervais, F. G., Cruz, R. P., Chateauneuf, A. *et al.* 2001. Selective modulation of chemokinesis, degranulation, and apoptosis in eosinophils through the $PGD_2$ receptors CRTH2 and DP. *J. Allergy Clin. Immunol.* 108:982.
12 Satoh, T., Moroi, R., Aritake, K. *et al.* 2006. Prostaglandin D2 plays an essential role in chronic allergic inflammation of the skin via CRTH2 receptor. *J. Immunol.* 177:2621.
13 Chevalier, E., Stock, J., Fisher, T. *et al.* 2005. Cutting edge: chemoattractant receptor-homologous molecule expressed on Th2 cells plays a restricting role on IL-5 production and eosinophil recruitment. *J. Immunol.* 175:2056.
14 Matsuoka, T., Hirata, M., Tanaka, H. *et al.* 2000. Prostaglandin D2 as a mediator of allergic asthma. *Science* 287:2013.
15 Beltrani, V. S. 1999. The clinical spectrum of atopic dermatitis. *J. Allergy Clin. Immunol.* 104:S87.
16 Leung, D. Y. 1999. Pathogenesis of atopic dermatitis. *J. Allergy Clin. Immunol.* 104:S99.
17 Iwasaki, M., Nagata, K., Takano, S., Takahashi, K., Ishii, N. and Ikezawa, Z. 2002. Association of a new-type prostaglandin D2 receptor CRTH2 with circulating T helper 2 cells in patients with atopic dermatitis. *J. Invest. Dermatol.* 119:609.
18 Hijnen, D., Nijhuis, E., Bruin-Weller, M. *et al.* 2005. Differential expression of genes involved in skin homing, proliferation, and apoptosis in CD4+ T cells of patients with atopic dermatitis. *J. Invest. Dermatol.* 125:1149.
19 Spergel, J. M., Mizoguchi, E., Brewer, J. P., Martin, T. R., Bhan, A. K. and Geha, R. S. 1998. Epicutaneous sensitization with protein antigen induces localized allergic dermatitis and hyperresponsiveness to methacholine after single exposure to aerosolized antigen in mice. *J. Clin. Invest.* 101:1614.
20 He, R., Oyoshi, M. K., Jin, H. and Geha, R. S. 2007. Epicutaneous antigen exposure induces a Th17 response that drives airway inflammation after inhalation challenge. *Proc. Natl Acad. Sci. USA* 104:15817.
21 Wang, G., Savinko, T., Wolff, H. *et al.* 2007. Repeated epicutaneous exposures to ovalbumin progressively induce atopic dermatitis-like skin lesions in mice. *Clin. Exp. Allergy* 37:151.
22 Lucaks, N., Berlin, A. A., Franz-Bacon, K. *et al.* 2008. CRTH2 antagonism significantly ameliorates airway hyperreactivity, and down-regulates inflammation-induced genes in a mouse model of airway inflammation. *Am. J. Physiol. Lung Cell. Mol. Physiol.,* in press.
23 Sásik, R., Woelk, C. H. and Corbeil, J. 2004. Microarray truths and consequences. *J. Mol. Endocrinol.* 33:1.
24 Cole, S. W., Galic, Z. and Zack, J. A. 2003. Controlling false-negative errors in microarray differential expression analysis: a PRIM approach. *Bioinformatics* 19:1808.
25 Boehme, S. A., Sullivan, S. K., Crowe, P. D. *et al.* 1999. Activation of mitogen-activated protein kinase regulates eotaxin-induced eosinophil migration. *J. Immunol.* 163:1611.
26 Cookson, W. 2004. The immunogenetics of asthma and eczema: a new focus on the epithelium. *Nat. Rev. Immunol.* 4:978.
27 Gabrielson, T. O., Dale, I., Brandtzaeg, P. *et al.* 1986. Epidermal and dermal distribution of a myelocytic antigen (L1) shared by epithelial cells in various inflammatory skin diseases. *J. Am. Acad. Dermatol.* 15:173.
28 Mork, G., Schjerven, H., Mangshau, L., Soyland, E. and Brandtzaeg, P. 2003. Proinflammatory cytokines upregulate expression of calprotectin (L1 protein, MRP-8/MRP-14) in cultured human keratinocytes. *Br. J. Dermatol.* 149:484.
29 Sugiura, H., Ebise, H., Tazawa, T. *et al.* 2005. Large-scale DNA microarray analysis of atopic skin lesions shows overexpression of an epidermal differentiation gene cluster in the alternative pathway and lack of protective gene expression in the cornified envelope. *Br. J. Dermatol.* 152:146.
30 Nomiya, R., Okano, M., Fujiwara, T. *et al.* 2008. CRTH2 plays an essential role in the pathophysiology of Cry j 1-induced pollinosis in mice. *J. Immunol.* 180:5680.
31 Takeshita, K., Yamasaki, T., Akira, S., Gantner, F. and Bacon, K. B. 2004. Essential role of MHC II-independent CD4+ T cells, IL-4 and STAT6 in contact hypersensitivity induced by fluorescein isothiocyanate in the mouse. *Int. Immunol.* 16:685.
32 Campbell, J. J. 2005. Commentary 1: animal models of chemokine/receptor involvement in cutaneous T-lymphocyte homing. *Exp. Dermatol.* 14:76.
33 Cataisson, C., Pearson, A. J., Tsien, M. Z. *et al.* 2006. CXCR2 ligands and G-CSF mediate PKCalpha-induced intraepidermal inflammation. *J. Clin. Invest.* 116:2757.
34 Flier, J., Boorsma, D. M., Bruynzeel, D. P. *et al.* 1999. The CXCR3 activating chemokines IP-10, Mig, and IP-9 are expressed in allergic but not in irritant patch test reactions. *J. Invest. Dermatol.* 113:574.
35 Mischke, D., Korge, B. P., Marenholz, I., Volz, A. and Ziegler, A. 1996. Genes encoding structural proteins of epidermal cornification and S100 calcium binding proteins from a gene complex (''epidermal differentiation complex'') on human chromosome 1q21. *J. Invest. Dermatol.* 106:989.
36 Nomura, I., Gao, B., Boguniewicz, M., Darst, M. A., Travers, J. B. and Leung, D. Y. 2003. Distinct patterns of gene expression in skin lesions of atopic dermatitis and psoriasis: a gene microarray analysis. *J. Allergy Clin. Immunol.* 112:1195.
37 Marshall, D., Hardman, M. J., Nield, K. M. and Byrne, C. 2001. Differentially expressed late constituents of the epidermal cornified envelope. *Proc. Natl Acad. Sci. USA* 98:13031.
38 Loser, K. and Beissert, S. 2007. Dendritic cells and T cells in the regulation of cutaneous immunity. *Adv. Dermatol.* 23:307.
39 Volpe, E., Servant, N., Zollinger, R. *et al.* 2008. A critical function for transforming growth factor-beta, interleukin 23 and proinflammatory cytokines in driving and modulating human T(H)-17 responses. *Nat. Immunol.* 9:650.
40 Zhou, L., Ivanov, I. I., Spolski, R. *et al.* 2007. IL-6 programs T(H)-17 cell differentiation by promoting sequential engagement of the IL-21 and IL-23 pathways. *Nat. Immunol.* 8:967.
41 Liu, Y. J., Soumelis, V., Watanabe, N. *et al.* 2007. TSLP: an epithelial cell cytokine that regulates T cell differentiation by conditioning dendritic cell maturation. *Annu. Rev. Immunol.* 25:193.
42 Soumelis, V., Reche, P. A., Kanzler, H. *et al.* 2002. Human epithelial cells trigger dendritic cell mediated allergic inflammation by producing TSLP. *Nat. Immunol.* 3:673.
43 Kabashima, K., Shiraishi, N., Sugita, K. *et al.* 2007. CXCL12-CXCR4 engagement is required for migration of cutaneous dendritic cells. *Am. J. Pathol.* 171:1249.